Collective dynamics of accelerated atoms

Benedikt Richter[1,2,3], Hugo Terças[1,4], Yasser Omar[1,2], and Inés de Vega[3]

[1]*Instituto de Telecomunicações, Lisbon, Portugal*
[2]*Instituto Superior Técnico, Universidade de Lisboa, Portugal*
[3]*Arnold Sommerfeld Center for Theoretical Physics, Department für Physik,*
Ludwig-Maximilians-Universität München, Germany and
[4]*Instituto de Plasmas e Fusão Nuclear, Lisbon, Portugal*
(Dated: May 2, 2017)

We study the collective dynamics of accelerated atoms interacting with a massless field via an Unruh-deWitt type interaction. We first derive the general Hamiltonian describing such a system and then, employing a Markovian master equation, we study the corresponding collective dynamics. In particular, we observe that the emergence of entanglement between two-level atoms is linked to the building up of coherences between them and to superradiant emission. Furthermore, we propose an experimental setup for a quantum simulation of this system using Bose-Einstein condensates, where the two-level atoms are realized by optical tweezers and the condensate's Bogoliubov modes play the role of the Unruh radiation.

I. INTRODUCTION

The vacuum perceived by a non-inertial observer is by no means a boring place. For instance, it is well-known that an accelerated observer coupled to the vacuum experiences it as a thermal field [1] and that a pair of accelerated atoms starting from a separable state can become entangled [2–5]. Furthermore, it is known that for entangled states entanglement can be degraded due to acceleration, as described for non-localized Fock states [6–9] and for localized Gaussian states [10]. As expected from the equivalence principle, the creation and the degradation of entanglement can also be observed in curved spacetimes [11–14]. Also, acceleration can affect the interactions between two atoms [15, 16].

In order to analyze these effects, the accelerated atoms are often considered as an open quantum system coupled to a quantum field, which therefore plays the role of an environment [17, 18]. With this approach, the evolution equation of the atomic reduced density operator – also known as the master equation – can be computed by considering a weak coupling between the atoms and their surrounding field [19–21]. In such master equations, the action of the field in the atomic dynamics is encoded in the dissipative rates, which in turn depend on a sum over environment fluctuations defining the environment correlation function. In this regard, most earlier approaches were based on taking a Wightman correlation function which describe the environment fluctuations as seen from the laboratory frame of reference [4, 20, 21].

In contrast to this, in this paper we consider Rindler spacetime to re-express the Hamiltonian of a collection of accelerated atoms within the frame of reference of one of them. This allows to explicitly incorporate in the Hamiltonian the red-shifts between atoms having different accelerations. In addition, our representation shows that for atoms equally accelerated we recover the Hamiltonian corresponding to standing atoms coupled to a thermal reservoir, as expressed via a thermofield transformation [22]. Hence, our approach provides more physical insight

than previous ones, as it allows comparing the case of accelerated atoms in vacuum with the case of atoms in a thermal field at the Hamiltonian level, i.e. without having to compare the dynamics corresponding to the two cases. Furthermore, the derived Hamiltonian describes an arbitrary number N of atoms coupled to a massless field via an Unruh-deWitt interaction. This general form enables us to investigate collective effects such as superrandiance and to analyze the emergence of entanglement beyond the commonly considered case of only two accelerated atoms [2, 4, 19, 20].

To illustrate our formalism we analyze the dynamics of a collection of N atoms both when they are all equally accelerated and when they have different accelerations. In this context, we explore the conditions for the emergence of cooperative phenomena and coherent emission. Moreover, considering a Markov and a secular approximation we obtain a Lindblad master equation, which allows us to compute entanglement between the atoms based on a well defined (i.e. positive) reduced density operator. We find that entanglement is indeed built along the evolution and persists in the long time limit, an observation that is consistent with previous studies of two uniformly accelerated atoms [19]. However, our approach allows us to show that the entanglement itself is not due to the acceleration, which merely produces the effect of a thermal bath in the case of equal accelerations, but rather it is due to the presence of a common environment for the atoms.

For the accelerations that can be achieved in laboratories, relativistic effects such as the ones described above are generally small [23]. Therefore, experiments employing analogue systems are more promising candidates to observe these phenomena. Proposed platforms for such experiments include circuit QED [24, 25], superconducting qubits [26] and cold atoms [27]. For the Unruh effect, in particular, an analogue experiment utilizing a Bose-Einstein condensate was proposed [28]. Here, the derived Hamiltonian for the Rindler modes enables us to propose a new implementation to simulate the collective

dynamics of a collection of accelerated atoms based on Bose-Einstein condensates. The key idea is to model the field by the Bogoliubov excitations of the Bose-Einstein condensate and to use optical tweezers to produce artificial two-level atoms.

The outline of the paper is the following. In Sec. II, we introduce the framework that is used in the present work, and derive the Hamiltonian describing a system of N accelerated two-level atoms[1] coupled to a scalar field. In Sec. III, we derive the master equation governing the time evolution of the atoms, while in Sec. IV we consider such an equation to analyze the atom dynamics for different representative cases. Furthermore, we propose an experimental setup to simulate the open system dynamics in Bose-Einstein condensates in Sec. V. Finally, in Sec. VI we draw the conclusions from this work.

II. FRAMEWORK FOR ACCELERATED ATOMS

In this work we consider the setting of several two-level systems, which we refer to as atoms, interacting with a massless scalar field at zero temperature, i.e., in the vacuum state. Assuming that the atoms are initially in the ground state and move in some arbitrary inertial motion, it is clear that the system remains in its ground state and no correlations between the atoms can emerge. However, if the atoms are in uniformly accelerated motion this statement does not remain true. From the perspective of an observer traveling together with one of the atoms, the field is no longer in the ground state but in an excited state. Therefore, a single atom being accelerated can become excited [1] and several atoms interacting with the same field can become correlated [2, 19]. In the following, we study a framework suitable to describe this situation. In particular, we derive the Hamiltonian governing the evolution of many accelerated atoms.

A. Scalar field in Rindler spacetime

Before moving to the case of Rindler spacetime, we briefly recall some properties of scalar fields in Minkowski spacetime. Let ϕ be a massless scalar field confined to a box of length L obeying the Klein-Gordon equation $\Box\phi = 0$, where $\Box$ denotes the d'Alembert operator. Then we can expand the field in a complete set of solutions

$$\phi = \sum_k \left(a_k u_k(x,t) + a_k^\dagger u_k^*(x,t) \right), \tag{1}$$

where the $u_k(x,t)$ are plane-wave solutions of the Klein-Gordon equation that are created and annihilated by the

operators $a_k^\dagger$ and a_k, respectively. However, in the following, we choose to expand the field ϕ in a different complete set of modes that is motivated by the setting we are considering in this work.

Rindler coordinates are suitable to describe an accelerated observer [29, 30]. In these coordinates an uniformly accelerated object is at rest. Here we discuss the $1+1$ dimensional case, i.e., we neglect the orthogonal Euclidean directions usually labelled by y and z. The metric reads in conformal coordinates

$$ds^2 = e^{2\frac{a\xi}{c^2}} \left(c^2 d\tau^2 - d\xi^2 \right), \tag{2}$$

where τ is the time-like and ξ the space-like coordinate and a is a parameter with the dimension of acceleration. The range of τ and ξ in each of the wedges is $(-\infty,\infty)$. In Minkowski coordinates the world-line (x,ct) of a particle moving with constant proper acceleration is given by

$$x = \pm \frac{c^2}{a} e^{\frac{a\xi}{c^2}} \cosh\left(\frac{a\tau}{c}\right), \tag{3a}$$

$$ct = \frac{c^2}{a} e^{\frac{a\xi}{c^2}} \sinh\left(\frac{a\tau}{c}\right), \tag{3b}$$

where the sign $\pm$ depends on the direction of acceleration; see Fig. 1. The proper acceleration α is related to the acceleration parameter a, as $\alpha = a\exp(-a\xi/c^2)$. In consequence, the spatial coordinate ξ is constant and dictated by α.

Considering for instance two particles with proper accelerations α_1 and α_2, one obtains the world-lines (x_1,ct_1) and (x_2,ct_2), parametrized by the coordinate time τ that equals the proper time of particle 1 for $\xi_1 = 0$, as

$$(x_1,ct_1) = c^2 \alpha_1 \left(\pm\cosh\left(\frac{\alpha_1\tau}{c}\right), \sinh\left(\frac{\alpha_1\tau}{c}\right) \right), \tag{4a}$$

$$(x_2,ct_2) = c^2 \alpha_2 \left(\pm\cosh\left(\frac{\alpha_2\tau}{c}\right), \sinh\left(\frac{\alpha_2\tau}{c}\right) \right). \tag{4b}$$

In (4), without loss of generality, we have chosen the spacial coordinate of particle 1 to be zero, $\xi_1 = 0$. In consequence, α_1 coincides with the acceleration parameter a and it may seem that α_2 or equivalently the world-line (x_2,ct_2) depends on $\alpha_1 = a$. However, that is not the case as ξ_2 is fixed by the proper acceleration of particle 2, $\alpha_2 = a\exp(-a\xi_2/c^2)$. Therefore, α_2 and α_1 are two independent parameters. What we have done to arrive at (4) is to choose a particular value for the, a priori, unphysical parameter a to obtain a simple form of the world-lines.

Next, we consider the quantization of a massless scalar field ϕ in this spacetime[2]; see [29] for details. A scalar field in a box (size L) with periodic boundary conditions can be expanded as

$$\phi = \sum_k \left(b_k^{\mathrm{I}} u_k^{\mathrm{I}}(\xi,\tau) + b_k^{\mathrm{II}} u_k^{\mathrm{II}}(\xi,\tau) \right) + \text{ h.c.}, \tag{5}$$

---

[1] In the literature these are sometimes referred to as Unruh-deWitt detectors.

[2] We work in units where $\hbar = k_B = 1$ and keep the speed of light c explicit.

(a) Counter-accelerating atoms.
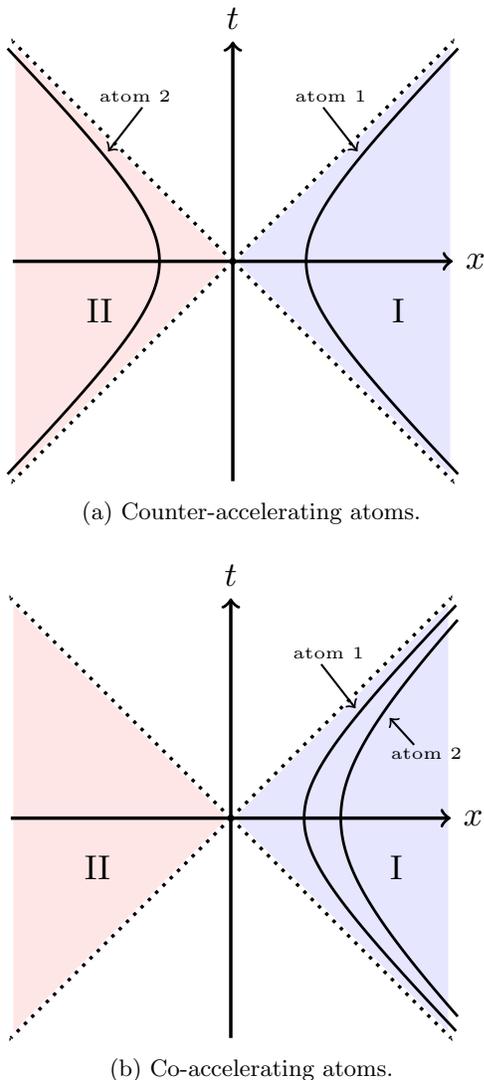

(b) Co-accelerating atoms.

FIG. 1: Schematic figure showing atoms interacting with a massless scalar field. The ground state of the field is maximally entangled between regions I and II. Therefore, the reduced vacuum state in either of the regions is given by a thermal state. In Figure (a), the two atoms are in anti-parallel accelerated motion and interact with the massless field supported in causally disconnected regions of spacetime. In Figure (b), the two atoms are accelerated in parallel and therefore only interact with the field in region I.

where

$$u_k^{\mathrm{I}}(\xi,\tau) = \frac{1}{\sqrt{2L|k|}} e^{i(k\xi - |k|c\tau)}, \quad \text{in region I,} \quad (6a)$$

$$u_k^{\mathrm{II}}(\xi,\tau) = \frac{1}{\sqrt{2L|k|}} e^{i(k\xi + |k|c\tau)}, \quad \text{in region II} \quad (6b)$$

are solutions of $\Box\phi = 0$, where $\Box$ denotes the d'Alembert operator. The solutions are delta normalized, $(u_k^\Lambda, u_l^{\Lambda'}) = \delta(k-l)\delta_{\Lambda,\Lambda'}$, $(u_k^\Lambda, u_l^{\Lambda'*}) = 0$ with $\Lambda, \Lambda' \in \{\mathrm{I}, \mathrm{II}\}$. The

time-like Killing vectors in regions I and II are given by ∂_τ and $\partial_{-\tau}$ and act on the solutions as $\partial_\tau u_k^{\mathrm{I}}(\xi,\tau) = -i|k|cu_k^{\mathrm{I}}(\xi,\tau)$ and $\partial_{-\tau} u_k^{\mathrm{II}}(\xi,\tau) = -i|k|cu_k^{\mathrm{II}}(\xi,\tau)$, i.e., these are the positive frequency solutions. The free field Hamiltonian $H^{\mathrm{I/II}}$ in each of the wedges is given by $H^{\mathrm{I/II}} = \sum_k |k|cb_k^{\mathrm{I/II}\dagger}b_k^{\mathrm{I/II}}$. Therefore, the vacuum state in each of the regions I/II is given by $H^{\mathrm{I/II}}|0\rangle_{\mathrm{I/II}} = 0$ and the global vacuum can be written as $|0\rangle_{\mathrm{R}} = |0\rangle_{\mathrm{I}} \otimes |0\rangle_{\mathrm{II}}$. To obtain the complete free field Hamiltonian H_{f} one has to take care of the fact that time is running in different directions in the two regions. Therefore, the Hamiltonian contains a relative minus sign

$$H_{\mathrm{f}} = H^{\mathrm{I}} - H^{\mathrm{II}} = \sum_k |k|c\left(b_k^{\mathrm{I}\dagger}b_k^{\mathrm{I}} - b_k^{\mathrm{II}\dagger}b_k^{\mathrm{II}}\right). \quad (7)$$

Alternatively, the field ϕ can also be expanded in a complete set of solutions of the Klein-Gordon equation for Minkowski spacetime. One finds that the Minkowski (M) vacuum $|0\rangle_{\mathrm{M}}$ is related to the Rindler (R) vacuum by

$$|0\rangle_{\mathrm{M}} = S|0\rangle_{\mathrm{R}}, \quad (8)$$

where the operator S acts as

$$S^\dagger b_k^{\mathrm{I/II}} S = \cosh(r_k) b_k^{\mathrm{I/II}} + \sinh(r_k) b_k^{\mathrm{II/I}\dagger}, \quad (9)$$

where r_k is defined by $\tanh(r_k) = e^{-\frac{\pi c^2|k|}{a}}$. In consequence, the Minkowski vacuum expressed in Rindler modes according to (8) reads

$$|0\rangle_{\mathrm{M}} = \prod_k \frac{1}{\cosh(r_k)} \sum_{n=0}^\infty \tanh(r_k)^n |n_k\rangle_{\mathrm{I}} \otimes |n_k\rangle_{\mathrm{II}}. \quad (10)$$

That is, the Minkowski vacuum written in Rindler modes exhibits entanglement between regions I and II. State (10) is also referred to as thermofield double state. It is the purification of a thermal state in region I by modes of region II. Therefore taking the partial trace over one of the regions results in a thermal state of the Unruh temperature $T_{\mathrm{U}} \sim \alpha$, where α is the proper acceleration of the observer [29].

B. Hamiltonian for accelerated atoms

In the following we derive the Hamiltonian governing the evolution of N two-level atoms with rotating frequencies ω_i coupled to a massless scalar field by an Unruh-DeWitt type coupling [29]. The interaction is described by an interaction Hamiltonian of the form

$$H_I^{(i)} = \chi(\tau_i)Q(\tau_i)\phi[x(\tau_i)], \quad (11)$$

where $\chi(\tau_i)$ is the coupling that might be chosen to be constant ($\chi(\tau_i) = \chi = \text{const.}$), $Q(\tau_i)$ is the monopole moment of the ith atom and $x(\tau_i)$ is its trajectory. The full

Hamiltonian for atom i, that generates the time translations with respect to the proper time τ_i of the atom, in the Schrödinger picture is given by

$$H = \frac{d\tau}{d\tau_i} H_{\mathrm{f}} + H_{\mathrm{S}}^{(i)} + H_I^{(i)}, \tag{12}$$

where $H_{\mathrm{S}}^{(i)} = \omega_i \hat{\sigma}_i^+ \hat{\sigma}_i^-$ is the Hamiltonian describing the internal degrees of freedom of the ith atom with $\hat{\sigma}^+ = \frac{1}{2}(\hat{\sigma}_x + i\hat{\sigma}_y)$ and $\hat{\sigma}^- = \frac{1}{2}(\hat{\sigma}_x - i\hat{\sigma}_y)$, $H_I^{(i)}$ gives the atom-field interactions, H_{f} is the free field Hamiltonian (7), τ is the time coordinate, and τ_i is the proper time of the atom. A priori, there is no preferred mode expansion for the field ϕ. The expansion in Minkowski modes, Eq. (1), as well as the expansion in Rindler modes, Eq. (5), are both legitimate choices that are equivalent. In this work, contrary to, e.g. [4], we choose to formulate the Hamiltonian governing the evolution using the expansion in Rindler modes. We consider the atoms moving along the world-lines $(\xi(\tau_i), \tau(\tau_i))$ introduced in (3), where $\xi(\tau_i) = \xi_i$ is fixed by the proper acceleration α_i according to $\alpha_i = a \exp(-a\xi_i/c^2)$ and the time coordinate reads $\tau = \tau_i \exp(-a\xi_i/c^2)$. Thus, we identify the red-shift

$$\frac{d\tau}{d\tau_i} = e^{-\frac{a\xi_i}{c^2}}, \tag{13}$$

and thus, the red-shifted frequencies are defined as

$$\Omega_i = \frac{d\tau_i}{d\tau} \omega_i. \tag{14}$$

We aim at investigating the general setting of N atoms coupled to a common scalar field ϕ according to (11). Therefore, the Hamiltonian (12) has to be generalized to describe more than one atom. It is clear that the free field Hamiltonian H_{f} remains unchanged, while the contribution to the energy from the internal dynamics of the atoms is given by the sum of the individual energies described by $H_{\mathrm{S}}^{(i)}$, i.e. the total contribution H_{S} is given by $H_{\mathrm{S}} = \sum_i H_{\mathrm{S}}^{(i)}$. Finally, we have to take care of the individual interaction terms (11). Also for these, the total interaction energy is given by the sum $H_I = \sum_i H_I^{(i)}$. Therefore, considering N atoms, we can write the Hamiltonian in the Schrödinger picture with respect to the time τ as

$$H^{(S)} = \sum_k |k| c b_k^{\mathrm{I}\dagger} b_k^{\mathrm{I}} - \sum_k |k| c b_k^{\mathrm{II}\dagger} b_k^{\mathrm{II}}$$
$$+ \sum_{i=1}^{N_{\mathrm{I}}} \Omega_i \hat{\sigma}_i^+ \hat{\sigma}_i^- - \sum_{i=1}^{N_{\mathrm{II}}} \Omega_i \hat{\sigma}_i^+ \hat{\sigma}_i^-$$
$$+ \sum_{i=1}^{N_{\mathrm{I}}} \sum_k \frac{d\tau_i}{d\tau} \frac{g_{k,i}}{\sqrt{2L|k|}} \left(\hat{\sigma}_i^+ + \hat{\sigma}_i^- \right) \left(b_k^{\mathrm{I}} e^{ik\xi_i} + b_k^{\mathrm{I}\dagger} e^{-ik\xi_i} \right)$$
$$- \sum_{i=1}^{N_{\mathrm{II}}} \sum_k \frac{d\tau_i}{d\tau} \frac{g_{k,i}}{\sqrt{2L|k|}} \left(\hat{\sigma}_i^+ + \hat{\sigma}_i^- \right) \left(b_k^{\mathrm{II}} e^{ik\xi_i} + b_k^{\mathrm{II}\dagger} e^{-ik\xi_i} \right), \tag{15}$$

where the first N_{I} atoms accelerate in positive direction and the remaining ones accelerate in negative direction, i.e., they live in wedges I and II, respectively. Further, we defined $g_{k,i}(\tau_i) = \chi(\tau_i) g_{k,i} = \chi g_{k,i}$, where $g_{k,i}$ is the usual coupling appearing in $Q(\tau_i)$.

Since, throughout this work, we are interested in atoms coupled to a scalar field in the Minkowski vacuum, we frequently encounter vacuum expectation values $\langle H_{\mathrm{R}} \rangle_{\mathrm{M}}$ of some Hamiltonian H_{R}, defined with respect to Rindler modes. Therefore, it is convenient to absorb the transformation S, relating Minkowski and Rindler vacua, into the Hamiltonian and to define transformed Hamiltonians H_{R}' by

$$\langle H_{\mathrm{R}} \rangle_{\mathrm{M}} = \langle S^\dagger H_{\mathrm{R}} S \rangle_{\mathrm{R}} = \langle H_{\mathrm{R}}' \rangle_{\mathrm{R}}, \tag{16}$$

where the action of S is given in (9). The free Hamiltonian transforms trivially, $H_{\mathrm{f}}' = H^{\mathrm{I}} - H^{\mathrm{II}} = H_{\mathrm{f}}$. The interaction Hamiltonians $H_I^{(i)}$, however, are not invariant and pick up non-trivial contributions. The transformation of the Hamiltonian $H^{(S)}$ can be performed straight forwardly. The same goes through very similarly for the Hamiltonian in the interaction picture, where we first transform using the operator S and, subsequently, we go to the interaction picture

$$\langle H^{(S)} \rangle = \langle 0 | S e^{iH_0\tau} H^{(I)'} e^{-iH_0\tau} S^\dagger | 0 \rangle, \tag{17}$$

where we introduced the definition

$$H^{(I)'} = e^{-iH_0\tau} S^\dagger H^{(S)} S e^{iH_0\tau}. \tag{18}$$

Using expression (15) for $H^{(S)}$ and definition (18), one obtains for the Hamiltonian in the interaction picture

$$H^{(I)'} = \sum_{i=1}^{N_{\mathrm{I}}} \frac{d\tau_i}{d\tau} \left[\sum_k \frac{g_{k,i}}{\sqrt{2L|k|}} \left(\hat{\sigma}_i^+ e^{i\Omega_i\tau} + \mathrm{h.c.} \right) \times \right.$$
$$\times \left(\cosh(r_k) \left(b_k^{\mathrm{I}} e^{i(k\xi_i - |k|c\tau)} + b_k^{\mathrm{I}\dagger} e^{-i(k\xi_i - |k|c\tau)} \right) \right.$$
$$\left. \left. + \sinh(r_k) \left(b_k^{\mathrm{II}} e^{i(k\xi_i + |k|c\tau)} + b_k^{\mathrm{II}\dagger} e^{-i(k\xi_i + |k|c\tau)} \right) \right) \right] +$$
$$- \sum_{i=1}^{N_{\mathrm{II}}} \frac{d\tau_i}{d\tau} \left[\sum_k \frac{g_{k,i}}{\sqrt{2L|k|}} \left(\hat{\sigma}_i^+ e^{-i\Omega_i\tau} + \mathrm{h.c.} \right) \times \right.$$
$$\times \left(\cosh(r_k) \left(b_k^{\mathrm{II}} e^{i(k\xi_i + |k|c\tau)} + b_k^{\mathrm{II}\dagger} e^{-i(k\xi_i + |k|c\tau)} \right) \right.$$
$$\left. \left. + \sinh(r_k) \left(b_k^{\mathrm{I}} e^{i(k\xi_i - |k|c\tau)} + b_k^{\mathrm{I}\dagger} e^{-i(k\xi_i - |k|c\tau)} \right) \right) \right]. \tag{19}$$

This Hamiltonian describes an ensemble of $N = N_{\mathrm{I}} + N_{\mathrm{II}}$ atoms of which N_I are accelerated in one direction and the remaining N_{II} are accelerated in the opposite direction. In general, each atom might experience a (different) arbitrary uniform acceleration, such that our chosen reference frame moving with atom 1 sees their frequencies

red-shifted according to (14). In addition, we have defined

$$\sinh(r_k)^2 = \frac{1}{e^{\beta c|k|} - 1} \equiv n(k), \qquad (20a)$$

$$\cosh(r_k)^2 = \frac{1}{1 - e^{-\beta c|k|}} = 1 + n(k), \qquad (20b)$$

in terms of the inverse Unruh temperature $\beta = \frac{2\pi c}{\alpha_1}$. Written in this suggestive form, (20a) gives the Bose-Einstein distribution at inverse temperature β. Furthermore, our description allows us to see that when all atoms are equally accelerated the Hamiltonian (19) is exactly equivalent to the one describing a collection of $N = N_I$ atoms located at positions $\xi_i > 0$ within a line and coupled to a common thermal field in $1+1$ dimensions, once such field is treated with thermofield (also known as thermal Bogoliubov) transformation [22, 31, 32].

Having established the Hamiltonians (15) and (19), we now move on to study the dynamics of the system of accelerated atoms coupled to a massless scalar field. For this purpose, in the next Section we derive the respective master equations that govern such evolution in different cases, while in Sec. IV we use this equation to numerically analyze the dynamics of up to six atoms accelerating in the same direction.

III. MASTER EQUATION

We derive the master equation obtained by considering a second order perturbative expansion in the coupling Hamiltonian between the atoms and the scalar field. As discussed in Appendix A 1, this equation reads as follows,

$$\frac{d\rho_s(t)}{dt} = -\int_0^t d\tau \mathrm{Tr}_B\{[V_t^0 H_I, [V_\tau^0 H_I, \rho_B^{\mathrm{eq}} \otimes \rho_s(t)]]\}. \qquad (21)$$

In this Section, we consider two main situations: all atoms accelerating in the same direction, and then some atoms accelerating in the opposite direction.

A. Co-accelerating atoms

We insert the Hamiltonian (19) with $N_I = N$ atoms accelerated in one direction and $N_{II} = 0$ atoms accelerated in the opposite one in the master equation (21). Then, we perform the trace over the environment and consider a change of variables in the time-integrals $t - \tau \to \tau$, such that the resulting equation can be written as

$$\frac{d\rho_s(t)}{dt} = \sum_{i,j} \sum_{\xi,\eta=+,-} \gamma_{ij}^{\eta\xi}(t)[\hat{\sigma}_j^\eta \rho_s(t), \hat{\sigma}_i^\xi] + \mathrm{h.c.} \qquad (22)$$

with the coefficients $\gamma_{ij}^{\eta\xi}(t)$ defined as

$$\gamma_{nl}^{\eta\xi}(t) = \int_0^t d\tau C_{nl}(\tau) e^{-\eta i\Omega_l(t-\tau)} e^{\xi i \Omega_n t}. \qquad (23)$$

The correlation functions $C_{nl}(\tau)$ read

$$C_{nl}(t-\tau) = \alpha_{nl}^{\mathrm{I}}(t-\tau) + \alpha_{nl}^{\mathrm{II}}(t-\tau), \qquad (24)$$

with

$$\alpha_{nj}^{\mathrm{I}}(t-\tau) = \sum_k \chi_{nj} \cosh^2(r_k) e^{ik(\xi_n - \xi_j)} e^{-i|k|c(t-\tau)},$$

$$\alpha_{nj}^{\mathrm{II}}(t-\tau) = \sum_k \chi_{nj} \sinh^2(r_k) e^{ik(\xi_n - \xi_j)} e^{i|k|c(t-\tau)}, \quad (25)$$

where we have defined $\chi_{nj} = \left(\frac{d\tau_n}{d\tau}\right)\left(\frac{d\tau_j}{d\tau}\right) g_{kn} g_{kj}$.

We now consider the Markov approximation in the master equation (22), which implies that the integral limits of the coefficients (23) is extended to infinity [17, 18]. As further detailed in Appendix A 2, within this limit the coefficients $\gamma_{jn}^{\eta\xi}(t = \infty)$ can be written as

$$\gamma_{jn}^{+-} = g^{+-}\delta(\Omega_j - \Omega_n) e^{ik_{0j}(\xi_j - \xi_n)}(1 + \mathrm{sign}(\Delta_{nj})),$$

$$\gamma_{jn}^{-+} = g^{-+}\delta(\Omega_j - \Omega_n) e^{ik_{0j}(\xi_j - \xi_n)}(1 + \mathrm{sign}(\Delta_{nj})), \quad (26)$$

where we have introduced the notation $\gamma_{jn}^{+-} = \gamma_{jn}^{+-}(\infty)$, $\gamma_{jn}^{-+} = \gamma_{jn}^{-+}(\infty)$. In addition, we have defined $\Delta_{nj} = tc - (\xi_j - \xi_n)$, $g^{+-} = g\chi_{nj}(n(k_{0j})+1)$, $g^{-+} = g\chi_{nj} n(k_{0j})$, and the resonant wave-vector $k_{0j} = \Omega_j/c$, while the number of excitations in the field is given by the Bose-Einstein distribution (20a).[3] In terms of these coefficients, the Markovian master equation can be written, back in the Schrödinger picture as

$$\frac{d\rho_s(t)}{dt} = -i[H_S, \rho_s(t)] + \sum_{i,j} \gamma_{ij}^{+-}[\hat{\sigma}_j^+ \rho_s(t), \hat{\sigma}_i^-]$$

$$+ \sum_{i,j} \gamma_{ij}^{-+}[\hat{\sigma}_j^- \rho_s(t), \hat{\sigma}_i^+] + \mathrm{h.c.}. \qquad (27)$$

In contrast to the second order master equation (22) which does not preserve positivity of $\rho_s(t)$, Eq. (27) is in the Lindblad form and therefore preserves not only the trace and the hermiticity, but also the positivity of the reduced density matrix. This is an important property that shall be required if we want to calculate quantities such as entanglement.

_____

[3] Unlike in higher dimensions, the rates (26) do not decay with the distance r_{jn} between atoms j and n. This can naively be understood in analogy with an electric field $E = \nabla\varphi$ (φ: electric potential). A consequence of Gauss's law in d spacelike dimensions is that ∇E scales with the distance r as $\nabla E \sim r^{1-d}$ and, therefore, in one dimension, E is constant in regions with vanishing charge density. We note however, that the factor $1 + \mathrm{sign}(\Delta_{nj})$ ensures that causality is respected, in the sense that atoms only become connected through the field - so that the rates $\gamma_{jn}^{\gamma\xi}$ are non-zero - once their effective separation becomes time-like.

B. Counter-accelerating atoms

Following the same steps as in Sec. III A, we find, for atoms accelerating in different directions, that their reduced density matrix obeys the master equation

$$
\frac{d\rho_s(t)}{dt} = \sum_{i,j} \sum_{\xi \neq \eta = +,-} \gamma_{ij}^{\eta\xi}(t)[\hat{\sigma}_j^\eta \rho_s(t), \hat{\sigma}_i^\xi]
$$
$$
+ \sum_{\kappa,\gamma} \sum_{\xi \neq \eta = +,-} \gamma_{\kappa\gamma}^{\eta\xi}(t)[\hat{\sigma}_\gamma^\eta \rho_s(t), \hat{\sigma}_\kappa^\xi]
$$
$$
- \sum_{i,\kappa} \sum_{\xi = \eta = +,-} \gamma_{\kappa i}^{\eta\xi}(t)[\hat{\sigma}_i^\eta \rho_s(t), \hat{\sigma}_\kappa^\xi]
$$
$$
- \sum_{i,\kappa} \sum_{\xi = \eta = +,-} \gamma_{i\kappa}^{\eta\xi}(t)[\hat{\sigma}_\kappa^\eta \rho_s(t), \hat{\sigma}_i^\xi] + \text{h.c.}, \quad (28)
$$

where the coefficients $\gamma_{...}^{\eta\xi}(t)$ are defined similarly to the ones in the case of parallel acceleration, as detailed in Appendix A 3. In the long time limit, we find that the equation shall be written as

$$
\frac{d\rho_s(t)}{dt} = \sum_{i,j} \gamma_{ij}^{+-}(t)[\hat{\sigma}_j^+ \rho_s(t), \hat{\sigma}_i^-]
$$
$$
+ \sum_{i,j} \gamma_{ij}^{-+}(t)[\hat{\sigma}_j^- \rho_s(t), \hat{\sigma}_i^+] + \sum_{i,j} \gamma_{\kappa\gamma}^{+-}(t)[\hat{\sigma}_\gamma^+ \rho_s(t), \hat{\sigma}_\kappa^-]
$$
$$
+ \sum_{i,j} \gamma_{\kappa\gamma}^{-+}(t)[\hat{\sigma}_\gamma^- \rho_s(t), \hat{\sigma}_\kappa^+] - \sum_{i,\kappa} \gamma_{\kappa i}^{+-}(t)[\hat{\sigma}_i^+ \rho_s(t), \hat{\sigma}_\kappa^-]
$$
$$
- \sum_{i,\kappa} \gamma_{\kappa i}^{-+}(t)[\hat{\sigma}_i^- \rho_s(t), \hat{\sigma}_\kappa^+] - \sum_{i,\kappa} \gamma_{i\kappa}^{+-}(t)[\hat{\sigma}_\kappa^+ \rho_s(t), \hat{\sigma}_i^-]
$$
$$
+ \sum_{i,\kappa} \gamma_{i\kappa}^{-+}(t)[\hat{\sigma}_\kappa^- \rho_s(t), \hat{\sigma}_i^+] + \text{h.c.}, \quad (29)
$$

where we have defined $\gamma_{ij}^{-+}(t)$, $\gamma_{ij}^{++}(t)$, $\gamma_{\kappa\gamma}^{+-}(t)$ and $\gamma_{\kappa\gamma}^{-+}(t)$ as in Eq. (26), and

$$
\gamma_{\kappa i}^{+-} = \tilde{g}^{+-}\delta(\Omega_i - \Omega_\kappa)e^{ik_{0i}(\xi_i - \xi_\kappa)}(1 + \text{sign}(\Delta_{i\kappa})),
$$
$$
\gamma_{i\kappa}^{-+} = \tilde{g}^{-+}\delta(\Omega_j - \Omega_n)e^{ik_{0i}(\xi_j - \xi_n)}(1 + \text{sign}(\Delta_{nj})), \quad (30)
$$

with $\tilde{g}_{\kappa i}^{+-} = \tilde{g}_{\kappa i}^{-+} = \chi_{\kappa i}\sqrt{n(k_{0i})}\sqrt{1 + n(k_{0i})}$ and $\tilde{g}_{i\kappa}^{+-} = \tilde{g}_{i\kappa}^{-+} = \chi_{i\kappa}\sqrt{n(k_{0i})}\sqrt{1 + n(k_{0i})}$. We note that the cross-rates (30) for counter-accelerating atoms are in general non-vanishing and may give rise to entanglement as described in [3, 4].

IV. EXAMPLE WITH SIX ATOMS

Having developed all the necessary tools, in this Section we analyze the collective dynamics of up to six two-level atoms as viewed from the instantaneous rest frame of the atom $j = 1$. We consider for simplicity that all atoms are accelerated in the same direction, such that $N = N_I$ in the Hamiltonian (19), and that the reference atom has a frequency $\omega_1 = \omega_s$.

In Figs. 2 and 3 we consider additionally that atoms have the same acceleration. As it can be seen in the top panel of Fig. 2, the population of the reference atom $j = 1$

$$
P_1(t) = \langle \Psi_0 | \hat{\sigma}_1^+(t)\hat{\sigma}_1^-(t) | \Psi_0 \rangle, \quad (31)
$$

evolves up to a steady state which contains a finite population in the excited level. Such population is higher the higher the acceleration is. Moreover, the form of the Hamiltonian (19) shows that when all atoms are equally accelerated their dynamics as seen from their instantaneous rest frame is exactly equivalent to that of a set of atoms coupled to a thermal field with an inverse temperature $\beta = 2\pi/\alpha_1$, once it is expressed with a thermofield transformation [22, 31, 32]. However, in general the steady state achieved is not a thermal state $\rho_s^{th} = e^{-\beta H_s}/Z_s$. Indeed, even if the thermal state is a fixed point of the master equation (27) it is not its only possible steady state due to the presence of symmetries in the system [33]. This can be confirmed by analyzing the spectrum of the Lindblad superoperator $\mathcal{L}$ corresponding to such equation (27) when written in the vector form, i.e. $d\rho_s/dt = \mathcal{L}\rho_s$. In more detail, when the zero eigenvalue of $\mathcal{L}$ is degenerated, there is no unique steady state. As a consequence, different initial states will evolve into different steady states, and not necessarily to a single and unique (in this case thermal) steady state. In our case of a collection of atoms coupled to a common field, the zero eigenvalue of $\mathcal{L}$ is degenerated, and therefore the system does not always thermalize. We note also that such degeneracy is only removed when the emission rates of the equation are such that $\gamma_{lj}^{\eta\xi} \sim \delta_{lj}\gamma_{ll}^{\eta\xi}$, so that the atoms are virtually coupled to independent environments and evolve independently from the others.

The fact that atoms are coupled to a common environment has also important consequences in the emission rate

$$
R_{\text{tot}}(t) = -\frac{dP_{\text{tot}}(t)}{dt} = -\sum_{j=1}^N \frac{d\langle \hat{\sigma}_j^+ \hat{\sigma}_j^- \rangle}{dt}, \quad (32)
$$

where $P_{\text{tot}}(t) = (1/N)\sum_j P_j(t)$ and $P_j(t)$ is the population of the atom j. As it can be observed in the bottom panel of Fig. 2, the atomic emission rate has a negative slope at initial times, which is is typical from superradiance [34, 35]. As it can also be observed, such slope as well as the location of the superradiant peak (given by the maximum of $R(t)$) is highly dependent on the value of the atomic acceleration. In general, it can be concluded that collective effects are stronger (and therefore the superradiant peak occurs later) the smaller the acceleration is.

The presence of collective effects in the emission is related to the building up of coherences in the atomic system. Such coherences can be quantified in many different ways, like for instance by considering the sum of the off-diagonal elements of the reduced density matrix as
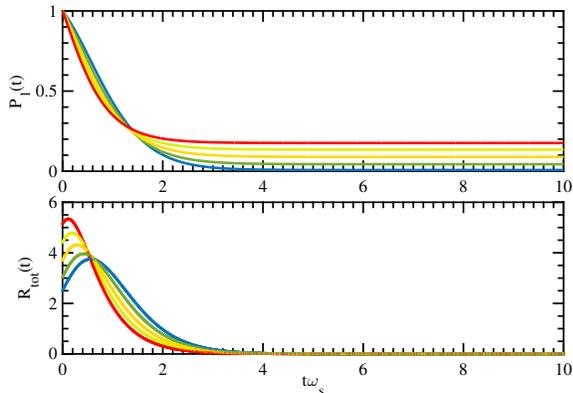
FIG. 2: Evolution of the atomic population (top panel) and emission rate (bottom panel) for $N = 6$ atoms at the same acceleration. The different curves correspond to increasing values of the acceleration $\alpha = 2, 4, 6, 8, 10$ in a rainbow scale going from red to blue curves. In the top panel, higher velocities have also higher values of the long time limit population, while in the lower panel, higher accelerations correspond to a higher maximum in the emission rate.

proposed in [36],

$$C_{\text{coh}}(t) = \sum_{j \neq l} |\langle \hat{\sigma}_j^+ \hat{\sigma}_l^- \rangle|. \tag{33}$$

In turn, coherences are also related to the generation of entanglement in the atomic ensemble. We consider here the concurrence for a pair of atoms of the ensemble $j = 1, 2$. As described in [37], the concurrence is defined as

$$C(\rho_s) = \max\{0, \lambda_1 - \lambda_2 - \lambda_3 - \lambda_4\}, \tag{34}$$

and the λ_i's are the eigenvalues, in decreasing order, of the Hermitian matrix $R = \sqrt{\sqrt{\rho_s} \tilde{\rho}_s \sqrt{\rho_s}}$, with $\tilde{\rho}_s = (\sigma_y^1 \otimes \sigma_y^2) \rho_s^* (\sigma_y^1 \otimes \sigma_y^2)$, where ρ_s^* is the complex conjugated of the reduced density matrix.

Fig. 3 displays the evolution of the coherences (top panel) and the concurrence (bottom panel) for the same value of accelerations as in Fig. 2. In general, coherences are built up in the system around the time at which the emission rates achieve their maximum. However, the persistence of such coherences in the steady state is more significant the higher the acceleration is. In addition, the amount of entanglement encoded in such coherences, as quantified by the concurrence, presents also a growth at initial times of the evolution and shows a higher maximum the smaller the acceleration is. In contrast, at longer times the entanglement appears to be more persistent for accelerations $\alpha \geq 4$.

When the atoms experience different accelerations their dynamics can no longer be mapped to that of atoms coupled to a common thermal radiation field. Instead, as shown in Fig. 4, they present features that are unique
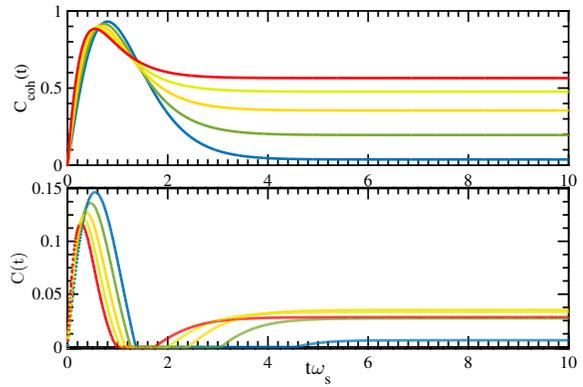

FIG. 3: Evolution of the atomic coherences (top panel) and concurrence (bottom panel) for $N = 6$ atoms at the same acceleration. The different curves correspond to increasing values of the acceleration $\alpha = 2, 4, 6, 8, 10$ (red to blue curves). In both panels, the curves with higher acceleration have lower maximum than the ones with lower acceleration.

to such system. Focusing in particular on the dynamics of the emission rate and the concurrence, we analyze in these figures the following situations: (a) all atoms having the same acceleration (as considered in the previous Figures 2 and 3) $\alpha = 2$; (b) all atoms j having different accelerations given by

$$\alpha_j = 0.2 + \Delta\alpha(j - 1), \tag{35}$$

where we have defined $\Delta\alpha$ as an acceleration mismatch parameter. We also consider that all atoms have the same frequency $\omega_j = \omega_1$, such that $\Omega_j \neq \Omega_l$ for any $j \neq l$. In this case, the decaying rates (26) are such that $\gamma_{lj}^{\eta\xi} \sim \delta_{lj} \gamma_{ll}^{\eta\xi}$, and each atom evolves independently to the others and relax to a thermal state. Finally, in (c) we consider the case where all atoms have different accelerations but we chose $\omega_j = \exp(-a\xi_j/c^2)\omega_1$, such that $\Omega_j = \Omega_1 = \omega_1$. With such a resonant condition, even when the atoms are accelerated differently, the rates $\gamma_{lj}^{\eta\xi}$ are also non-vanishing for $l \neq j$ and collective effects are still present in the dynamics. However, as shown by Fig. 4 such collective effects disappear when the acceleration mismatch $\Delta\alpha$ is too large.

After studying the collective dynamics of accelerated atoms, in the next Section, we give a proposal for its quantum simulation.

V. PROPOSAL FOR SIMULATION IN BOSE-EINSTEIN CONDENSATES

Analyzing the physics of the accelerated atomic ensemble described in the previous Sections is experimentally challenging. This is because for accelerations that can be achieved in laboratories, relativistic effects are typically
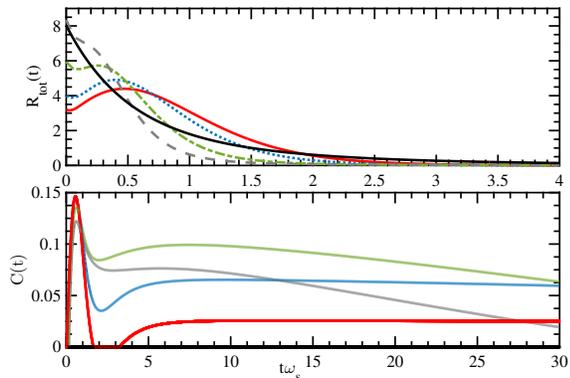
FIG. 4: Evolution of the emission rate (top panel) and concurrence (bottom panel) for different acceleration distributions, and considering all atoms initially excited. Solid red and solid black curves correspond, respectively, to the cases (a) where all atoms have the same acceleration $\alpha = 2$ and (b), where all atoms have different accelerations given by Eq. (35) with $\Delta\alpha = 0.6$ and $\omega_j = \omega_1 = 1$ for all j. The dashed green and dotted blue curves corresponds to the case (c) where atoms have different accelerations as given by Eq. (35), with $\Delta\alpha = 0.6$ and $\Delta\alpha = 0.03$ respectively. In this case the atomic frequencies are chosen such that $\Omega_j = \omega_1 = 1$.

negligibly small. Therefore, we consider in this Section an experimentally feasible scheme to simulate this system. We consider a Bose-Einstein condensate (BEC), which plays the role of the radiation field, and a set of impurities immersed in the BEC, which play the role of two-level atoms. The impurities are affected by the potential of a set of optical tweezers, which provides the ability to tune their internal energies [38]. Alkali atom BECs are specially suited for the quantum simulation for two reasons. First, the excitation spectrum in the long-wavelength limit is linear, $\omega \sim k$, which naturally mimics Unruh radiation. Secondly, the kHz energy scale of the BEC is suitable to drive two-level atoms as created by optical tweezers, for which a large number of two-level systems can be created on demand, distributed with different energy gaps and relative spatial positions.

A. Bogoliubov excitations as Unruh radiation

We start by implementing the first term of Eq. (15). A bosonic field $\phi(x,t)$ in a quasi-one-dimensional Bose-Einstein condensate (BEC) is described by the following Hamiltonian

$$H_f = \int dx \; \phi^\dagger \left[-\frac{\hbar^2}{2m}\frac{\partial^2}{\partial x^2} - \mu + u_0\phi^\dagger\phi \right]\phi, \qquad (36)$$

where μ is the chemical potential, u_0 is the interaction strength and a_k is a bosonic operator satisfying the usual

commutation relation $[a_k, a_{k'}^\dagger] = \delta_{k,k'}$ [39]. In the following, we make use of the Bogoliubov approximation, which amounts to neglecting the depletion from the macroscopically occupied vacuum state $\langle\phi\rangle = \sqrt{n_0}$ is small, such that

$$\phi(x,t) = e^{-i\mu t/\hbar}\left[\sqrt{n_0} + \frac{1}{\sqrt{L}}\sum_k \left(a_k e^{ikx} + a_k^\dagger e^{-ikx}\right)\right]. \tag{37}$$

Plugging this into Eq. (36), we obtain

$$\begin{aligned}H_f = E_0 &+ \sum_k \epsilon_k a_k^\dagger a_k \\ &+ \frac{1}{2}u_0 n_0 \sum_{k\neq 0}\left(2a_k^\dagger a_k + a_k^\dagger a_{-k}^\dagger + a_k a_{-k}\right),\end{aligned} \tag{38}$$

where $E_0 = Nu_0n_0$ is a spurious energy shift, with N denoting the total number of particles in the BEC, and $\epsilon_k = \hbar^2 k^2/(2m)$. By performing a Bogoliubov-Valatin transformation of the form $a_k = u_k b_k + v_k^* b_{-k}^\dagger$, the condition of b_k being also a bosonic operator implies the normalization condition $|u_k|^2 - |v_k|^2 = 1$, and diagonalizes the Bogoliubov Hamiltonian (38) as

$$H_f = \pm\sum_k E_k b_k^\dagger b_k, \tag{39}$$

where $E_k = \sqrt{\epsilon_k(\epsilon_k + \mu)}$ is the energy spectrum. By identifying the positive (negative) energy excitations as propagating plane waves in region I (II) of the Rindler spacetime, we can immediately identify Eq. (39) with the first term appearing in the Hamiltonian (15).

B. Optical tweezers as tunable two-level systems

In order to emulate the Hamiltonian of the two-level systems (atoms), we make use of a set of optical tweezers, which can be located at different positions on demand. As we are about to see, the spatial distribution of the optical tweezers will simulate the location of the atoms in different positions in Rindler spacetime [40]. Let $\psi(x)$ denote the field of an auxiliary particle (impurity) inside the BEC. The corresponding Hamiltonian reads

$$H_S = \int dx \; \psi^\dagger \left[-\frac{\hbar^2}{2M}\frac{\partial^2}{\partial x^2} - V_0 e^{-x^2/w^2} \right]\psi, \qquad (40)$$

where V_0 represents the depth of the potential (associated with the laser intensity) and w is the potential width (i.e. the laser beam waist). By expanding the field in the form $\psi(x) = \sum_n \varphi_n(x)c_n$, where $\varphi_n(x)$ satisfies the Schrödinger equation $H_S\varphi_n(x) = \varepsilon_n\varphi_n(x)$ and c_n is a bosonic operator with algebra $[c_n, c_m^\dagger] = \delta_{n,m}$, we can evoke the WKB approximation in order to determine the number of bound states n_b as

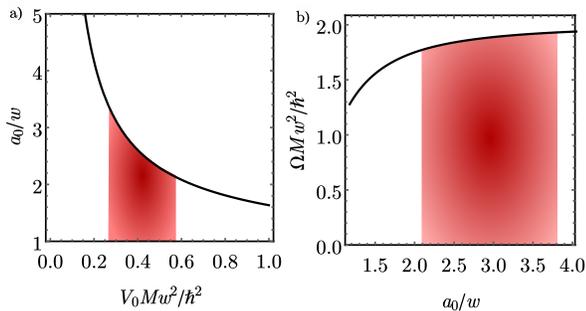$$n_b = \lfloor \frac{2}{\hbar^2}\sqrt{\frac{V_0 M}{\pi w}} - \frac{1}{2}\rfloor, \qquad (41)$$

FIG. 5: Panel a): Width of the bound states as a function of the optical tweezer potential depth. Panel b): Dependence of the atom energy on the bound state width. In both panel, the shadowed region corresponds to the two-level condition in Eq. (42).

with $\lfloor \cdot \rfloor$ denoting the integer part. We are mostly interested in the case where exactly two bound states can be produced ($n_b = 2$). By keeping the potential depth constant and tuning the the tweezer waist, for example, we obtain two-level atoms with energies in the range

$$\frac{4}{5\hbar^2}\sqrt{\frac{MV_0}{\pi}} < w < \frac{4}{3\hbar^2}\sqrt{\frac{MV_0}{\pi}}. \quad (42)$$

In that case, the two bound states $n = 0$ and $n = 1$ can be approximately described by the following variational wave functions,

$$\varphi_0(x) = \left(\frac{2}{\pi a_0^2}\right)^{1/4} e^{-x^2/a_0^2}, \quad \varphi_1(x) = 2\frac{x}{a_0}\varphi_0(x), \quad (43)$$

where a_0 is the width of the bound state, which can be related to the tweezer parameters as

$$\frac{w^2}{2a_0^2}\left(\frac{2}{a_0^2} + \frac{1}{w^2}\right)^3 = \frac{V_0^2 M^2 w^4}{\hbar^4}. \quad (44)$$

The variational energies are the given by $\varepsilon_n = \langle\varphi_n|H_S|\varphi_n\rangle$, and the two-level (atom) transition energy $\Omega = \varepsilon_1 - \varepsilon_0$ is given then given by

$$\Omega = \frac{2\hbar^2}{Ma_0^2} - \sqrt{2}V_0\frac{\sqrt{2a_0^4 + \frac{a_0^6}{w^2}}}{\left(a_0^2 + 2w^2\right)^2}. \quad (45)$$

Multiple atoms can therefore be simulated by tuning the width w_i of the different tweezers independently, which will then emulate the atoms' Hamiltonian in Eq. (15) provided the identification $\omega_i d\tau_i/d\tau \to \Omega_i$, yielding

$$H_S = \sum_i \Omega_i \sigma_i^+ \sigma_i^-, \quad (46)$$

where $\sigma_i^+ = c_{i,1}^\dagger c_{i,0}$ and $\sigma^- = c_{i,0}^\dagger c_{i,1}$.

C. System-bath interaction in the rotating-wave approximation

The interaction between a collection of two-level systems, created by the impurities trapped in the optical tweezers, and the phonons in the BEC is described by the following Hamiltonian

$$H_I = g\sum_i \int dx\, \psi^\dagger(x - x_i)\phi^\dagger(x)\phi(x)\psi(x - x_i), \quad (47)$$

where x_i is the location (in the laboratorial frame) of each optical tweezer and g is the atom-atom interaction strength ($g = u_0$ if the atoms and the reservoir are of the same species). By using the expansion in Eq. (38) and the two-level condition in (42), we obtain

$$H_I = H_I^{(0)} + H_I^{(1)} + H_I^{(2)}, \quad (48)$$

where $H_I^{(0)} = gn_0/L \sum_i \sum_{n=0}^1 c_{i,n}^\dagger c_{i,n}$ is the BEC Stark shift, which can be incorporated by a renormalizing the energy levels in the form $\varepsilon_n \to \varepsilon_n + gn_0$. The last term is second-order in the bosonic operators b_k, $\mathcal{O}(b_k^2)$, which we neglect in the spirit of the Bogoliubov approximation. Finally, the first-order term can be easily given as

$$H_I^{(1)} = \sum_k \sum_j \sum_{m,n=0}^1 \mathcal{G}_{ik}^{mn} e^{ikx_i} c_{i,m}^\dagger b_k c_{i,n} + \text{h.c.}, \quad (49)$$

where the components of the coupling tensor explicitly read

$$\mathcal{G}_{ik}^{00} = g\sqrt{\frac{n_0 S(k)}{L}} e^{-k^2 a_0^2/2}, \quad (50)$$

$$\mathcal{G}_{ik}^{11} = \left(1 - \frac{a_0^2 k^2}{2}\right)\mathcal{G}_{ik}^{00}, \quad \mathcal{G}_{ik}^{10} = \mathcal{G}_{ik}^{01*} = ia_0 k\mathcal{G}_{ik}^{00}.$$

Here, $S(k) = u_k - v_k$ denotes the BEC static structure factor within the Bogoliubov approximation. Eq. (49) contains intra-band ($m = n$) and inter-band ($m \neq n$) terms. However, intra-band couplings involve long wavelength phonons $k \sim 0$, for which $S(k) \sim 0$, and can therefore be neglected [41]. Moreover, we choose a narrow range of atom energies Ω_i for which the quasi-resonant k_i modes are located around the maximum of $|\mathcal{G}_{ik}^{01}|$ (see Fig. 6 for illustration). We then go to the interaction picture, as described above, to drop the terms proportional to $\sigma_i^+ b_k^\dagger$ and $\sigma_i^- b_k$. Within the RWA approximation, the interaction Hamiltonian finally reads

$$H_I^{\text{RWA}} \simeq \sum_{i,k} G_{ik} e^{ikx_i}\sigma_i^+ b_k + \text{h.c.}, \quad (51)$$

where $G_{ik} = \mathcal{G}_{ik}^{10}$. The latter is valid if the coupling between the optical tweezers and the BEC is sufficiently weak, i.e. provided the condition $g \ll u_0$. This is why a different species is necessary, allowing for g to be tuned via Feshbach resonances. The appropriate simulation of
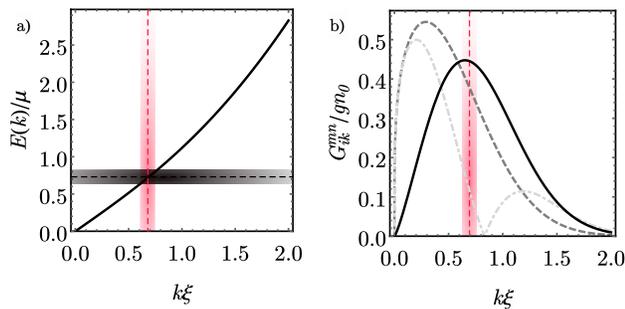
FIG. 6: Panel a): Dispersion relation of the Bogoliubov modes and the choice of the resonance value of the atoms. The horizontal (vertical) dashed line indicates the frequency (wave number) resonant with the central atom transition Ω. The shadowed horizontal (vertical) rectangle indicates the range of near-resonant frequencies (wave vectors) for a centred distribution of atom proper accelerations. Panel b): Strength of the couplings $|\mathcal{G}_{ik}^{00}|$ (dashed line), $|\mathcal{G}_{ik}^{11}|$ (dot-dashed line) and $|\mathcal{G}_{ik}^{10}|$ (solid line) near resonance. For illustration, we have used $a_0 = 2.2w$.

the system-bath reservoir in Eq. (15) is performed if we identify the laboratory positions x_i with the Rindler coordinates ξ_i and the matrix element G_{ik} with the term $g_{ik}d\tau_i/d\tau$.

Typical experimental setups with laser powers of ~ 800 mW result in potential depths of $V_0 \sim 2\pi \times 1$ kHz and beam waist of $w \sim 1.0$ μm [42]. The latter are comparable to the typical values of healing length ξ_{heal} and chemical potential μ in elongated ^{87}Rb condensates [43]. Moreover, the atoms could be constructed with ^{172}Yb atoms, which are heavy ($M/m \simeq 2$) and weakly-interacting enough (an estimate of the scattering lengths $a_{\text{Rb-Yb}} \sim -160.7a_{\text{Bohr}}$ and $a_{\text{Rb-Rb}} \sim 90.0a_{\text{Bohr}}$ yields $g \sim 0.18u_0$ [44, 45]) such that the approximations above hold (see Ref. [46] and references therein). In typical ^{87}Rb experiments with $n_0 \sim 50$ μm^{-1} (i.e. ~ 5000 atoms confined in a trap of size 100 μm [47]), and using the reasoning of Ref. [46], we estimate that retardation effects can be neglected for up to $N \sim 20$ atoms separated by $d \sim 2.8$ μm. In this case, hopping between the different tweezers can also be prevented.

VI. CONCLUSIONS

In this work we have studied the emergence of collective effects and entanglement in an ensemble of accelerated two-level atoms. We have derived a new Hamiltonian which describes the system in the accelerated frame of reference of one of the atoms. We have shown that, in the limit in which all atoms are equally accelerated, this Hamiltonian is exactly equivalent to the one describing a collection of N atoms coupled to a thermal field once such thermal field is treated with thermofield or thermal Bogoliubov transformation [22, 31, 32].

Our framework shows that the creation of coherences and entanglement between the two-level atoms is due to the fact that they are coupled to a common field, and not directly a consequence of their acceleration. Indeed, for atoms equally accelerated, the acceleration merely converts the surrounding field into an effective thermal field. In this regard, entanglement can be built even if the atoms are not accelerating (such that the effective temperature of the field is zero) provided that they are initially in an excited state (see discussion of entanglement generation in common fields in [18]). Obviously, entanglement can not be created if atoms are initially in their ground state and they have zero acceleration. Thus, acceleration – which leads to a finite temperature field – becomes a fundamental resource to create entanglement only in the case when the initial state of the atoms is the ground state.

However, when atoms undergo different accelerations the situation is more complex and the dynamics present features that do not correspond to the case of atoms coupled to a common thermal field. Thus, the physics of atoms experiencing different accelerations can not be observed in any other scenario than the relativistic one, unless a simulator is specifically designed for this purpose. We have given a concrete proposal for such a simulator of multiple accelerated atoms based on Bose-Einstein condensates. The key idea is to simulate the Unruh radiation field by the Bogoliubov modes (BEC excitations) and to implement the artificial atoms with optical tweezers. Interestingly, the later setup is not limited to the simulation of collective effects and entanglement generation but also offers the possibility to simulate other effects such as entanglement degradation in accelerated atoms.

MP1209.

Appendix A: Master equation

1. Derivation of the master equation

In this Appendix, we give the details of the derivation of the master equation (21) used in Sec. III.

The von Neumann equation for the density operator of the total system in the interaction picture, $\rho_{tot}^I(t)$, reads as follows:

$$\frac{d\rho_{\text{tot}}^I(t)}{dt} = \frac{1}{i}[V_t^0 H_I, \rho_{\text{tot}}^I(t)], \tag{A1}$$

where we have defined

$$V_{t-t_0}^0 H_I = \mathcal{U}_0^{-1}(t, t_0) H_I \mathcal{U}_0(t, t_0), \tag{A2}$$

and also $\rho_{\text{tot}}^I = \mathcal{U}_0^{-1}(t, t_0)\rho(t)\mathcal{U}_0(t, t_0)$ with the free evolution operator $\mathcal{U}_0(t, t_0) = e^{-iH_0(t-t_0)}$. To simplify the notation, we set $\rho_{\text{tot}}^I(t) = \rho(t)$. We can integrate (A1) between t_0 and t. After two iterations and a trace over the environmental degrees of freedom, this leads to the following equation,

$$\Delta\rho_s(t) = \frac{1}{i}\int_{t_0}^t d\tau \text{Tr}_B\{[V_\tau^0 H_I, \rho(t_0)]\} + \left(\frac{1}{i}\right)^2$$
$$\times \int_{t_0}^t d\tau \int_{t_0}^\tau d\tau' \text{Tr}_B\{[V_\tau^0 H_I, [V_{\tau'}^0 H_I, \rho(\tau')]]\}, \tag{A3}$$

where $\rho_s(t) = \text{Tr}_B\{\rho(t)\}$ is the system reduced density operator and

$$\Delta\rho_s(t) = \rho_s(t) - \rho_s(t_0). \tag{A4}$$

Eq. (A3) is exact, but some assumptions have to be made in order to express it as a closed equation for $\rho_s(t)$. For an initially uncorrelated state of the form $\rho(t_0) = \rho_s(t_0) \otimes \rho_B$, and considering the case where

$$\text{Tr}_B\{V_{t_0}^0 H_I \rho_B^{\text{eq}}\} = 0, \tag{A5}$$

the first term in (A3) can be eliminated. Note that this occurs for instance when the environment is initially in thermal equilibrium $\rho_B = \rho_B^{\text{eq}} = \frac{e^{-\beta H_B}}{\text{Tr}_B\{e^{-\beta H_B}\}}$.

After the change of variable $T = \tau$ and $s = \tau - \tau'$, Eq. (A3) becomes

$$\rho_s(t) = \rho_s(t_0) - \int_{t_0}^t dT \int_0^{T-t_0} d\tau \text{Tr}_B\{[V_T^0 H_I,$$
$$\times [V_{T-s}^0 H_I, \rho(t-\tau)]]\}. \tag{A6}$$

The evolution equation for the reduced density operator can be obtained by deriving (A6) with respect to t,

$$\frac{d\rho_s(t)}{dt} = -\int_0^{t-t_0} d\tau \text{Tr}_B\left\{[V_t^0 H_I, [V_{t-\tau}^0 H_I, \rho(t-\tau)]]\right\}, \tag{A7}$$

with initial condition $\rho_s(t_0)$. The density operator appearing in the right hand side of (A7) has the general form

$$\rho(t) = \rho_s(t) \otimes \rho_B(t) + \chi_{SB}(t). \tag{A8}$$

However, the term $\chi_{SB}(t)$, which describes the correlation between the system and the environment at time t, can be neglected with the assumption that $\tau_C \ll \Delta t$, where τ_C is the environment correlation time. Such time defines the time that the environment takes to return to its equilibrium state after interacting with the system, and therefore defines also the time scale at which system-environment correlations persist. Neglecting $\chi_{SB}(t)$ corresponds to the Born approximation, which is only valid up to order g^2 in the perturbation parameter [18, 48, 49]. Also, in order to transform the resulting equation into a time-local form, we further replace $\rho_s(t-\tau) = \rho_s(t)$ within the integral term. This approximation is valid provided that the system evolution time T_A is much slower than the correlation time of the environment τ_C, which settles the scale in which the integral decays. This is sometimes referred to as the first Markov approximation in the literature.

Choosing $t_0 = 0$, the evolution equation (A7) becomes, after a trivial change of variable $s \rightarrow t - \tau$,

$$\frac{d\rho_s(t)}{dt} = -\int_0^t d\tau \text{Tr}_B\{[V_t^0 H_I, [V_\tau^0 H_I, \rho_B(t) \otimes \rho_s(t)]]\}, \tag{A9}$$

where $\rho_B(t) = Tr_S\{\rho(t)\}$, and the initial condition is $\rho_s(0)$. This equation can be further simplified by considering that the environment always remains in its equilibrium state, $\rho_B(t) \approx \rho_B^{\text{eq}}$. Considering this, we find our basic model of equation to consider

$$\frac{d\rho_s(t)}{dt} = -\int_0^t d\tau \text{Tr}_B\{[V_t^0 H_I, [V_\tau^0 H_I, \rho_B^{\text{eq}} \otimes \rho_s(t)]]\}. \tag{A10}$$

2. The dissipative rates for co-accelerating atoms

Considering the long time limit of equation (22), implies that the integral limits of the coefficients (23) can be extended to infinity,

$$\gamma_{jn}^{+-}(\infty) = \int_0^\infty d\tau(\alpha_{jn}^{\text{I}}(t-\tau) + \alpha_{jn}^{\text{II}}(t-\tau))e^{i\Omega_j\tau - i\Omega_n t}$$
$$= \int_0^\infty d\tau(\alpha_{jn}^{\text{I}}(\tau) + \alpha_{jn}^{\text{II}}(\tau))e^{i\Omega_j\tau - i(\Omega_n - \Omega_j)t}$$
$$= \delta(\Omega_j - \Omega_n)\int_0^\infty d\tau \alpha_{jn}^{\text{I}}(\tau)e^{i\Omega_j\tau}, \tag{A11}$$

where we have considered that in the long time limit, $e^{i\Omega_j\tau - i(\Omega_n - \Omega_j)t}$ leads to a non-vanishing contribution only when the phase is zero, i.e. when $\Omega_n = \Omega_j$. Considering now that $\int_0^\infty dt e^{i\omega t} = \delta(\omega) + iP(1/\omega)$, and also

the definition (25) of the correlation function, we find

$$
\begin{aligned}
\gamma_{jn}^{+-}(\infty) = &\delta(\Omega_j - \Omega_n)\chi_{nj}\left[e^{ik_0(\xi_j-\xi_n)}J_j(k_0)(n(k_0)+1)\right.\\
&\left.-iP\int dk\chi_{nj}\left(\frac{e^{ik(\xi_j-\xi_n)}J_j(k)(n(k)+1)}{ck-\Omega_j}\right)\right],
\end{aligned}
$$
(A12)

where we have defined the resonant wave-vector $k_{0j} = \Omega_j/c$, and the spectral density $J_j(k) = \rho_{\text{DOS}}(k)g_j(k)^2$, with $\rho_{\text{DOS}}(k)$ the density of states. The principal value integral can be solved as

$$
\begin{aligned}
P\int dk\left(\frac{e^{ik(\xi_j-\xi_n)}J_j(k)(n(k)+1)}{ck-\Omega_j}\right) = &i\pi\text{sign}(\Delta_{nj})\times\\
&\times J_j(k_{0j})(n(k_{0j})+1),
\end{aligned}
$$
(A13)

where $\Delta_{nj} = tc - (\xi_j - \xi_n)$, and therefore,

$$
\gamma_{jn}^{+-}(\infty) = g^{+-}\delta(\Omega_j - \Omega_n)e^{ik_0(\xi_j-\xi_n)}(1+\text{sign}(\Delta_{nj})),
$$
(A14)

where we have defined the coupling strength $g^{+-} = g\chi_{nj}(n(k_0)+1)$ and $g_j = J_j(k_{0j}) \approx g$, provided that the spectral density is a smooth function in the frequency space. Hence, the principal value integral settles a causality condition that physically implies that dipole-dipole interactions only occurs within the light cone, i.e. at times $t > (\xi_j - \xi_n)/c$. In a similar way we find that

$$
\gamma_{jn}^{-+}(\infty) = g^{-+}\delta(\Omega_j - \Omega_n)e^{ik_0(\xi_j-\xi_n)}(1+\text{sign}(\Delta_{nj})),
$$
(A15)

where now $g^{-+} = g\chi_{nj}n(k_0)$. In addition, we have defined the number of excitations in the field as Eq. (20a).

3. The dissipative rates for counter-accelerating atoms

Here, we give the coefficients, $\gamma_{\cdots}^{\eta\xi}(t)$, appearing in the master equation counter-accelerating atoms, Eq. (29). We define the coefficients as

$$
\begin{aligned}
\gamma_{ij}^{\eta\xi}(t) &= \int_0^t d\tau C_{ij}(\tau)e^{\eta i\Omega_j(t-\tau)}e^{\xi i\Omega_i t},\\
\gamma_{i\kappa}^{\eta\xi}(t) &= \int_0^t d\tau C_{i\kappa}(\tau)e^{-\eta i\Omega_\kappa(t-\tau)}e^{\xi i\Omega_i t},\\
\gamma_{\kappa i}^{\eta\xi}(t) &= \int_0^t d\tau C_{\kappa i}(\tau)e^{\eta i\Omega_\kappa(t-\tau)}e^{-\xi i\Omega_i t},\\
\gamma_{\kappa\gamma}^{\eta\xi}(t) &= \int_0^t d\tau C_{\kappa\gamma}(\tau)e^{-\eta i\Omega_\gamma(t-\tau)}e^{-\xi i\Omega_\kappa t},
\end{aligned}
$$
(A16)

where the correlation functions C_{ij} appearing in Eq. (A16) are given by

$$
C_{ij}(t-\tau) = \alpha_{ij}^{\text{I}}(t-\tau) + \alpha_{ij}^{\text{II}}(t-\tau)
$$
(A17)

with

$$
\begin{aligned}
\alpha_{ij}^{\text{I}}(t-\tau) &= \sum_k \chi_{ij}\cosh^2(r_k)e^{-i|k|c(t-\tau)},\\
\alpha_{\kappa\gamma}^{\text{I}}(t-\tau) &= \sum_k \chi_{\kappa\gamma}\sinh^2(r_k)e^{-i|k|c(t-\tau)},\\
\alpha_{i\kappa}^{\text{I}}(t-\tau) &= \sum_k \chi_{i\kappa}\sinh(r_k)\cosh(r_k)e^{ik(\xi_i-\xi_\kappa)}e^{-i|k|c(t-\tau)},\\
\alpha_{ij}^{\text{II}}(t-\tau) &= \sum_k \chi_{ij}\sinh^2(r_k)e^{i|k|c(t-\tau)},\\
\alpha_{\kappa\gamma}^{\text{I}}(t-\tau) &= \sum_k \chi_{\kappa\gamma}\cosh^2(r_k)e^{i|k|c(t-\tau)},\\
\alpha_{i\kappa}^{\text{II}}(t-\tau) &= \sum_k \chi_{i\kappa}\sinh(r_k)\cosh(r_k)e^{ik(\xi_i-\xi_\kappa)}e^{i|k|c(t-\tau)}.
\end{aligned}
$$
(A18)

These satisfy the following properties: $\alpha_{\kappa i}^{\text{I}}(t-\tau) = \alpha_{\kappa i}^{\text{I}}(t-\tau) = (\alpha_{i\kappa}^{\text{I}}(t-\tau))^*$ and $\alpha_{\kappa i}^{\text{II}}(t-\tau) = \left(\alpha_{i\kappa}^{\text{II}}(t-\tau)\right)^*$.

[1] W. G. Unruh, Phys. Rev. D 14, 870 (1976).
[2] B. Reznik, Found. Phys. 33, 167 (2003), arXiv:quant-ph/0212044 [quant-ph].
[3] E. G. Brown, E. Martin-Martinez, N. C. Menicucci, and R. B. Mann, Phys. Rev. D 87, 084062 (2013), arXiv:1212.1973 [quant-ph].
[4] G. Salton, R. B. Mann, and N. C. Menicucci, New J. Phys. 17, 035001 (2015), arXiv:1408.1395 [quant-ph].
[5] M. Ahmadi, K. Lorek, A. Chęcińska, A. R. H. Smith, R. B. Mann, and A. Dragan, Phys. Rev. D 93, 124031 (2016), arXiv:1602.02349 [quant-ph].
[6] I. Fuentes-Schuller and R. B. Mann, Phys. Rev. Lett. 95, 120404 (2005), arXiv:quant-ph/0410172 [quant-ph].
[7] D. E. Bruschi, J. Louko, E. Martin-Martinez, A. Dragan, and I. Fuentes, Phys. Rev. A 82, 042332 (2010), arXiv:1007.4670 [quant-ph].
[8] B. Richter and Y. Omar, Phys. Rev. A 92, 022334 (2015), arXiv:1503.07526 [quant-ph].
[9] J. Wang and J. Jing, Phys. Rev. A 82, 032324 (2010).
[10] B. Richter, K. Lorek, A. Dragan, and Y. Omar, Phys. Rev. D 95, 076004 (2017), arXiv:1701.05906 [quant-ph].
[11] S. Kanno, J. P. Shock, and J. Soda, Phys. Rev. D 94, 125014 (2016), arXiv:1608.02853 [hep-th].
[12] A. G. S. Landulfo, Phys. Rev. D 93, 104019 (2016), arXiv:1603.06641 [gr-qc].
[13] G. Menezes, Phys. Rev. D 94, 105008 (2016), arXiv:1512.03636 [gr-qc].
[14] Y. Dai, Z. Shen, and Y. Shi, JHEP 09, 071 (2015), arXiv:1507.00612 [gr-qc].

[15] J. Marino, A. Noto, and R. Passante, Phys. Rev. Lett. **113**, 020403 (2014).

[16] L. Rizzuto, M. Lattuca, J. Marino, A. Noto, S. Spagnolo, W. Zhou, and R. Passante, Phys. Rev. **A 94**, 012121 (2016).

[17] H. Breuer and F. Petruccione, *The theory of Quantum Open Systems* (Oxford Univ. Press, Oxford, 2002).

[18] I. de Vega and D. Alonso, Rev. Mod. Phys. **89**, 015001 (2017), 1511.06994.

[19] F. Benatti and R. Floreanini, Phys. Rev. **A 70**, 012112 (2004).

[20] J. Hu and H. Yu, Phys. Rev. **A 91**, 012327 (2015), arXiv:1501.03321 [quant-ph].

[21] J. Zhang and H. W. Yu, Phys. Rev. **D 75**, 104014 (2007), arXiv:0705.1092 [gr-qc].

[22] I. de Vega and M.-C. Bañuls, Phys. Rev. A **92**, 052116 (2015).

[23] L. C. B. Crispino, A. Higuchi, and G. E. A. Matsas, Rev. Mod. Phys. **80**, 787 (2008).

[24] M. del Rey, D. Porras, and E. Martin-Martinez, Phys. Rev. **A 85**, 022511 (2012), arXiv:1109.0209 [quant-ph].

[25] N. Friis, A. R. Lee, K. Truong, C. Sabín, E. Solano, G. Johansson, and I. Fuentes, Phys. Rev. Lett. **110**, 113602 (2013).

[26] L. García-Álvarez, S. Felicetti, E. Rico, E. Solano, and C. Sabín, Sci. Rep. **7**, 657 (2017).

[27] J. Rodriguez-Laguna, L. Tarruell, M. Lewenstein, and A. Celi, Phys. Rev. **A 95**, 013627 (2017), arXiv:1606.09505 [cond-mat.quant-gas].

[28] A. Retzker, J. I. Cirac, M. B. Plenio, and B. Reznik, Phys. Rev. Lett. **101**, 110402 (2008).

[29] N. D. Birrell and P. C. W. Davies, *Quantum Fields in Curved Space*, Cambridge Monographs on Mathematical Physics (Cambridge Univ. Press, Cambridge, UK, 1984).

[30] S. Takagi, Prog. Theor. Phys. Suppl. **88**, 1 (1986).

[31] W. Israel, Phys. Lett. A **57**, 107 (1976).

[32] M. Blasone, P. Jizba, and G. Vitiello, *Quantum Field Theory and Its Macroscopic Manifestations Boson Condensation, Ordered Patterns and Topological Defects* (World Scientific Singapore, 2011).

[33] J. Thingna, D. Manzano, and J. Cao, Sci. Rep. **6**, 28027 (2016).

[34] I. de Vega, D. Porras, and J. I. Cirac, Phys. Rev. Lett. **101**, 260404 (2008).

[35] C. Navarrete-Benlloch, I. de Vega, D. Porras, and J. I. Cirac, New J. Phys. **13**, 023024 (2011).

[36] T. Baumgratz, M. Cramer, and M. B. Plenio, Phys. Rev. Lett. **113**, 140401 (2014).

[37] W. K. Wootters, Phys. Rev. Lett. **80**, 2245 (1998).

[38] P. H. Jones, O. M. Maragò, and G. Volpe, *Optical Tweezers: Principles and Applications* (Cambridge Univ. Press, Cambridge, UK, 2011).

[39] C. J. Pethick and H. Smith, *Bose-Einstein condensation in dilute gases* (Cambridge university press, 2002).

[40] H. Kim, W. Lee, H.-g. Lee, H. Jo, Y. Song, and J. Ahn, Nat. Comm. **7** (2016).

[41] A. Klein, M. Bruderer, S. R. Clark, and D. Jaksch, New J. Phys. **9**, 411 (2007).

[42] C. Muldoon, L. Brandt, J. Dong, D. Stuart, E. Brainis, M. Himsworth, and A. Kuhn, New J. Phys. **14**, 073051 (2012).

[43] J. Denschlag, J. E. Simsarian, D. L. Feder, C. W. Clark, L. A. Collins, J. Cubizolles, L. Deng, E. W. Hagley, K. Helmerson, W. P. Reinhardt, S. L. Rolston, B. I. Schneider, and W. D. Phillips, Science **287**, 97 (2000).

[44] M. Borkowski, P. S. Żuchowski, R. Ciuryło, P. S. Julienne, D. Kedziera, L. Mentel, P. Tecmer, F. Münchow, C. Bruni, and A. Görlitz, Phys. Rev. **A 88**, 052708 (2013).

[45] J. P. Burke and J. L. Bohn, Phys. Rev. **A 59**, 1303 (1999).

[46] T. Ramos, H. Pichler, A. J. Daley, and P. Zoller, Phys. Rev. Lett. **113**, 237203 (2014).

[47] P. Krüger, S. Hofferberth, I. E. Mazets, I. Lesanovsky, and J. Schmiedmayer, Phys. Rev. Lett. **105**, 265302 (2010).

[48] C. Cohen-Yannoudji, J. Dupont-Roc, and G. Grynberg, *Atom-Photon Interactions. Basic Processes and Applications* (Wiley Interscience, 1992).

[49] H.-P. Breuer, B. Kappler, and F. Petruccione, Phys. Rev. **A 59**, 1633 (1999).